Topological data analysis of continuum percolation with disks

Leo Speidel
Department of Statistics, University of Oxford, Oxford, United Kingdom
and Systems Biology Doctoral Training Centre, University of Oxford, Oxford, United Kingdom

Heather A. Harrington and S. Jonathan Chapman
Mathematical Institute, University of Oxford, Oxford, United Kingdom

Mason A. Porter
Department of Mathematics, University of California Los Angeles, Los Angeles, California 90095, USA

(Received 20 April 2018; published 31 July 2018)

We study continuum percolation with disks, a variant of continuum percolation in two-dimensional Euclidean space, by applying tools from topological data analysis. We interpret each realization of continuum percolation with disks as a topological subspace of $[0,1]^2$ and investigate its topological features across many realizations. Specifically, we apply persistent homology to investigate topological changes as we vary the number and radius of disks, and we observe evidence that the longest persisting invariant is born at or near the percolation transition.

DOI: 10.1103/PhysRevE.98.012318

I. INTRODUCTION

Percolation and its many variants are some of the most popular topics in statistical physics. They have been used in the study of a diverse variety of phenomena, ranging from biological and social contagions to connectivity of infrastructure [1–3]. Continuum percolation models can help provide mechanistic understanding for the formation of structures embedded in space and are closely related to spatially-embedded random graphs [4]. Understanding the properties of spatially-embedded random graphs has long been of theoretical interest [4–8], and it has numerous applications, such as for investigating properties of granular packings [9,10] and sensor networks [11–13].

Studying spatial percolation processes can be helpful for investigations of spatially-embedded systems, which is particularly important in light of the increased availability of rich, finely-grained data about such systems. For example, advances in imaging technology have led to increasingly accurate measurements of biophysical networks [14] (such as vascular networks, leaf-venation networks, bronchial trees in the lung, and neuronal networks), which—like many other networks and complex systems—are embedded in space [15,16]. The properties and formation mechanisms of biophysical networks have been investigated as optimization problems [17], and they have also been studied using fluid dynamics [18] and in relation to random processes, such as random sequential adsorption [19]. Some of these situations, such as flocks of *Volvox barberi* [20], also form fascinating packing structures.

In many continuum percolation models (and in percolation problems more generally [1,2]), there are known phase transitions (identified theoretically or computationally) as one varies the model parameters [4,5]. For instance, a large percolating cluster may emerge suddenly as smaller clusters connect to each other. Percolation transitions are interesting because they indicate a change in long-range spatial correlations. To detect such structural changes, one commonly studies changes in the sizes of connected clusters.

In the present paper, we take a different approach, as we focus instead on the *shape* of clusters. We perform computations to investigate changes in the topological[1] properties of clusters [21–23]. The extent to which varying model parameters affects topological properties has been examined in some classical models of statistical physics, such as in models of interacting spins [24–26], and we do this in our focal problem as well. Specifically, we study one-dimensional (1D) topological invariants, which one can interpret as cycles or holes in the structure of a point cloud of data (including data from a network). We examine what we call a "continuum percolation with disks," a variant of continuum percolation, in which we place N disks of radius r independently and uniformly at random in two-dimensional (2D) Euclidian space. This percolation model is related to random geometric graphs (RGGs) [4,6,12,27].

To identify topological invariants of continuum percolation with disks, we calculate its homology groups H_0 and H_1. The dimension of H_0 equals the number of connected components, and the percolation and connectivity transitions are phase transitions related to H_0. The percolation transition occurs in the regime $0 < \lim_{N\to\infty} Nr^2 < \infty$, and the connectivity transition occurs in the regime $\lim_{N\to\infty} Nr^2 = \infty$ [4]. The latter regime is thus in the supercritical regime of the percolation transition. One can interpret the dimension of H_1 as the number of cycles, in the form of 1D holes, in a structure. Previous studies have identified two topological phase transitions that are related to the first homology group H_1. They each

[1]We use the word "topology" in its standard mathematical sense, rather than in the sense of examining connectivity structure in networks ("graph topology" or "network topology"), although the latter is popular in network analysis.

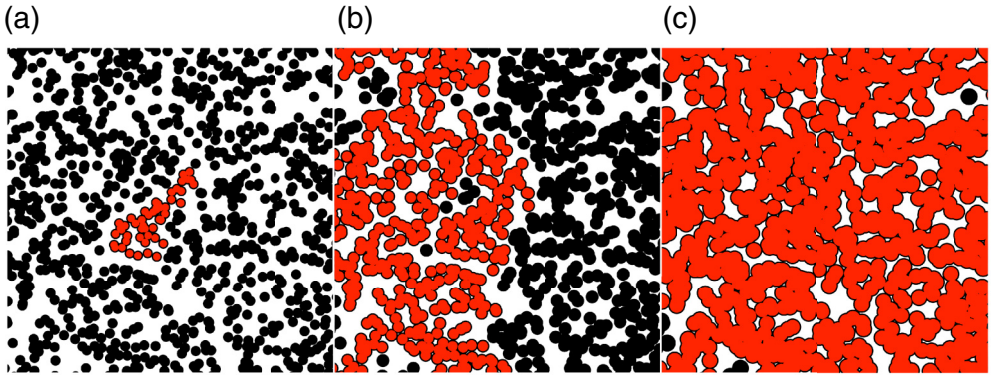

FIG. 1. One realization of continuum percolation with disks with filling factors of (a) $\eta(N,r) = 0.5$, (b) $\eta(N,r) = 1.128$, and (c) $\eta(N,r) = 1.5$, where $\eta(N,r) = N\pi r^2$ and there are $N = 1000$ disks of radius r. We show the largest connected cluster in red. It has been estimated that a percolation transition occurs at $\eta_c \approx 1.128$ [28].

correspond to a transition between zero and nonzero dimensions of H_1 [7,8]. The first phase transition occurs in the subcritical regime of the percolation transition (in which $\lim_{N\to\infty} Nr^2 = 0$), and the second phase transition occurs in the supercritical regime of the percolation transition.

It is partially understood how the first homology group changes in the critical regime of the percolation transition (see Sec. IV), but it is not well-understood how it changes at and near the percolation transition. We apply persistent homology (PH) [21,23] and study topological changes close to the percolation transition. Based on our calculations, the longest persisting topological invariant appears to be born at the percolation transition. This suggests that there is a change in the shapes (in addition to a change in the sizes) of clusters at the percolation transition.

The rest of our paper is organized as follows. First, we define continuum percolation more precisely and then define *continuum percolation with disks*. To help characterize continuum percolation with disks, we then discuss the sizes, number, and shapes of its clusters. We investigate continuum percolation with disks by computing PH and then conclude with a brief summary and discussion.

II. CONTINUUM PERCOLATION

Consider a metric space (X,d). Models of *continuum percolation* are random processes in which subsets $D_i \subseteq X$ (where $i \in \{1,\dots,N\}$) are chosen randomly with some probability distribution, resulting in a structure $\bigcup_{i=1}^{N} D_i$.

We consider the unit square $X = [0,1]^2$ equipped with the Euclidean metric d. We sample points $\boldsymbol{x}_i \in X$ (with $i \in \{1,\dots,N\}$) independently and uniformly at random, and we thereby obtain disks $D_i(r) = \{\boldsymbol{y} \in X : d(\boldsymbol{y},\boldsymbol{x}_i) < r\}$ of radius $r \geqslant 0$ that are centered at these points. The radius r is the same for all disks. The resulting structure $\mathcal{D}(r) = \bigcup_{i=1}^{N} D_i(r)$ is a union of potentially overlapping disks (see Fig. 1). We refer to this model as *continuum percolation with disks*.

A related model is a random geometric graph (RGG) [12,29]. To construct an RGG from a continuum-percolation model, one first defines a node set $V = \{1,\dots,N\}$ and an edge set $E = \{(i,j) : D_i \cap D_j \neq \varnothing\}$. One can induce an RGG from continuum percolation by placing nodes independently and uniformly at random in 2D Euclidean space and connecting pairs of nodes that lie within a specified distance $2r$ [6,27].

Both continuum percolation and RGGs have been studied extensively for many years (e.g., see the review [5] and references therein), with a focus on identifying and characterizing phase transitions [6,30] and relating continuum percolation to percolation on lattices [31]. Both continuum percolation and RGGs have been studied in a variety of metric spaces [4,16,27,32]. One can also choose different probability distributions for placing points; consider higher-dimensional spaces; and examine "softer" potentials (in contrast to the Heaviside function above), in which nodes are adjacent to each other with a probability that decays with increasing distance between them [12].

III. SIZES AND NUMBER OF CLUSTERS

One can partition any realization of the structure $\mathcal{D}(r)$ into disjoint clusters. The distributions of the number of clusters and the number of disks in the largest cluster depend on the combination of the parameters N and r.

It is useful to study $\eta(N,r) = N\pi r^2$, which is called the *filling factor*. The size of the largest cluster undergoes a phase transition as one varies $\eta(N,r)$. For $\lim_{N\to\infty} \eta(N,r) < \eta_c$, the size of the largest cluster is, with probability 1, at most $O(\ln N)$ of the number N of disks as $N \to \infty$. (See Theorem 10.3 in Ref. [4].) When $\lim_{N\to\infty} \eta(N,r)$ approaches the critical percolation transition value (i.e., the percolation "threshold") η_c from below, clusters merge until, at $\lim_{N\to\infty} \eta(N,r) = \eta_c$, there emerges a unique giant cluster (i.e., giant component) with size $O(N)$. (See Theorem 10.9 in Ref. [4].) Percolation transitions have been studied for many models and in numerous situations, including for lattice models and networks, for continuum models with various geometric objects, and in different dimensions [2,5,28,33–35]. For continuum percolation with disks, the exact value of the percolation threshold η_c is unknown. It has been estimated numerically to be $\eta_c \approx 1.128$ [28].

In the supercritical regime, for which $\lim_{N\to\infty} \eta(N,r) > \eta_c$, clusters keep merging as $\eta(N,r)$ increases. In a second ("connectivity") phase transition, which occurs for $\lim_{N\to\infty} \eta(N,r) = \infty$, all clusters merge into a single cluster with probability 1. The critical value for this connectivity

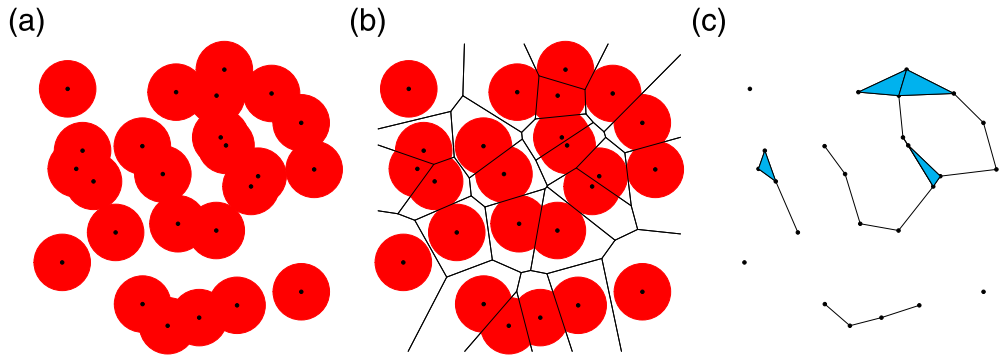

FIG. 2. (a) A realization of continuum percolation with disks with $N = 25$ and $r = 0.22$. (b) Voronoi tessellation that we construct using the centers of the disks in panel (a). (c) We construct an alpha complex from the information in panel (b). We represent 0-simplices by nodes, 1-simplices by edges (which connect adjacent nodes to each other), and 2-simplices by filled triangles. In this example, there are six clusters (so $\beta_0 = 6$) and one hole (so $\beta_1 = 1$).

transition satisfies [4]

$$\lim_{N\to\infty} \frac{\eta_c^{\text{connect}}(N,r)}{\ln(N)} = \frac{1}{4}. \tag{1}$$

IV. SHAPES OF CLUSTERS

We are interested in understanding the change in shape of connected clusters as we vary $\eta(N,r)$. To investigate this, we interpret $\mathcal{D}(r)$ as a topological subspace of (X,d) and study its topological properties. Specifically, we study its *homology groups*, which correspond, intuitively, to the numbers of holes in different dimensions [36].

We can calculate the homology groups of $\mathcal{D}(r)$ by studying a different topological space with homology groups that are isomorphic to those of $\mathcal{D}(r)$. The topological space $\mathcal{C}(r)$ that we study is the *alpha complex* [37], which is a type of *simplicial complex*. (See, e.g., Refs. [23,36] for the definition of a simplicial complex.) To construct an alpha complex, we calculate the Voronoi tesselation from the centers of the disks. We denote the intersection of a disk and its corresponding Voronoi cell by $V_i(r)$ (where $i \in \{1,\ldots,N\}$). The alpha complex $\mathcal{C}(r)$ includes 0-simplices $\{V_i(r)\}$ (where $i \in \{1,\ldots,N\}$) and k-simplices (with $k = 1$ and $k = 2$), given by $\{V_{i_0}(r),\ldots,V_{i_k}(r)\}$ such that $V_{i_0}(r) \cap \cdots \cap V_{i_k}(r) \neq \varnothing$. In our setting, the Nerve Theorem implies that $\mathcal{C}(r)$ and $\mathcal{D}(r)$ have the same homology (i.e., their homology groups are isomorphic) [21,38]. In Fig. 2, we visualize the alpha complex for a small example of continuum percolation with disks.

The kth homology group $H_k[\mathcal{C}(r)]$ describes the k-dimensional holes of $\mathcal{D}(r)$ [23,36]. The dimension of $H_k[\mathcal{C}(r)]$ is the kth Betti number β_k. The 0th Betti number β_0 is equal to the number of clusters. As we discussed in Sec. III, β_0 has been studied extensively in percolation (although typically without explicitly invoking ideas from homology). Intuitively, the first Betti number β_1 counts the number of holes. In this paper, we focus on β_1, which gives information about the shapes of the clusters.

Known phase transitions in the first Betti number

Theoretical work relating Betti numbers to continuum percolation indicates that the shapes of clusters change as one varies $\eta(N,r)$ [7,8]. For instance, it has been shown, for $\lim_{N\to\infty}\eta(N,r) = 0$, that there is a phase transition at which nontrivial 1D homology first appears. The critical value satisfies

$$\lim_{N\to\infty} \sqrt{N}\eta_c^{\text{exist}}(N,r) = c_{\text{exist}}. \tag{2}$$

Below the critical value, $\beta_1 = 0$; above the critical value, $\beta_1 > 0$ with probability 1. (See, e.g., Theorem 4.12 in Ref. [7].)

Similar to the connectivity transition in Eq. (1), the first Betti number vanishes for $\lim_{N\to\infty}\eta(N,r) = \infty$. The critical value for this phase transition satisfies (see, e.g., Theorem 4.12 in Ref. [7])

$$\lim_{N\to\infty} \frac{\eta_c^{\text{vanish}}(N,r)}{\ln(N)} = c_{\text{vanish}}. \tag{3}$$

In the critical regime, in which $\eta(N,r)$ approaches a finite and nonzero limit as $N \to \infty$, it is known that β_1 scales linearly in the number of disks:

$$\lim_{N\to\infty} \frac{E[\beta_1]}{N} = f(\eta) \tag{4}$$

for some function $f(\eta) \in (0,\infty)$. (See, e.g., Theorem 4.6 in Ref. [7].) Other than Eq. (4), it is not understood what happens at or near the percolation transition. In Sec. V, we confirm Eq. (4) with numerical computations (see Fig. 4) and investigate the behavior of $f(\eta)$ near the percolation transition.

V. PERSISTENT HOMOLOGY (PH) AND RESULTS

We aim to apply PH to characterize structural changes over a wide range of values of $\eta(N,r)$, especially near the percolation transition in the critical regime. PH is a method for topological data analysis of point clouds that extracts qualitative features over multiple scales [21,23,39], which we examine by varying the filling factor $\eta(N,r)$. PH has been used to investigate force networks in granular materials [40,41], to analyze functional brain networks [42], and for many other applications [23].

As we increase the value of r, we construct an alpha complex $\mathcal{C}(r)$. By increasing r, which causes $\eta(N,r)$ to change, we obtain a nested sequence (a so-called *filtration*) of simplicial complexes. Calculating PH of the filtration then allows us to examine how the features evolve with the filling factor $\eta(N,r)$.

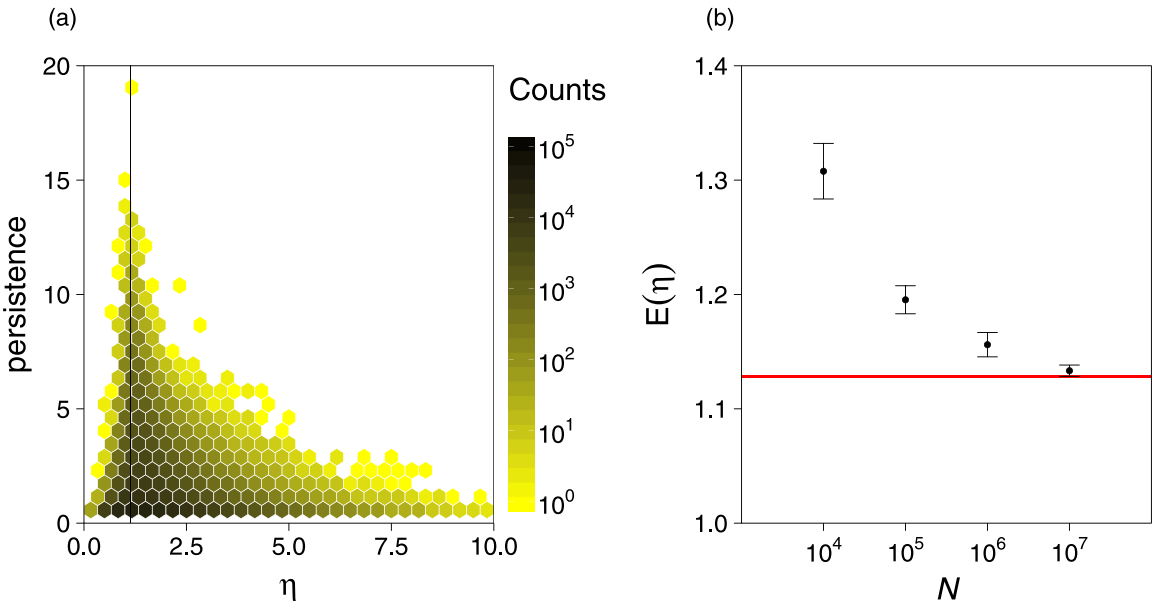

FIG. 3. (a) Birth–persistence diagram for 1D invariants of continuum percolation with disks with $N = 10^6$ disks. We summarize this diagram using a hexagonal binning. The vertical black line shows $\eta_c \approx 1.128$. (b) Mean value of η of the longest persisting 1D invariant for different values of N. The error bars indicate the 95% confidence intervals of the means, and the horizontal line indicates the percolation threshold ($\eta_c \approx 1.128$) for $N \to \infty$.

Based on the comparison of different implementations of PH by Otter *et al.* [23], we use the software package DIONYSUS [43]. (We tested that our results are qualitatively the same when we use the software package GUDHI [44].) The output from the software consists of pairs of birth and death values. After rescaling, these give the values of $\eta(N,r)$ at which a topological feature appears and disappears, respectively.

We visualize the output of PH using a birth–persistence diagram. In this diagram, we plot the persistence of an invariant, defined as the difference of the death and birth values of $\eta(N,r)$, versus the value of $\eta(N,r)$ at which the invariant feature is born. In Fig. 3(a), we show the birth–persistence diagram of one realization of continuum percolation with disks with $N = 10^6$ disks. We find that 95% of the invariants have a persistence that is less than 2.11 and that the mean $\eta(N,r)$ at birth is at approximately $\eta(N,r) = 1.6$, which is considerably larger than η_c. We observe an increasing trend in the persistence of the longest persisting invariants for $\eta(N,r) < \eta_c$ and a decreasing trend for $\eta(N,r) > \eta_c$. The longest persisting invariant is born near $\eta(N,r) \approx \eta_c$. [See the vertical line in Fig. 3(a).] In Fig. 3(b), we see that the longest persisting invariant is born progressively closer to η_c for larger N. This

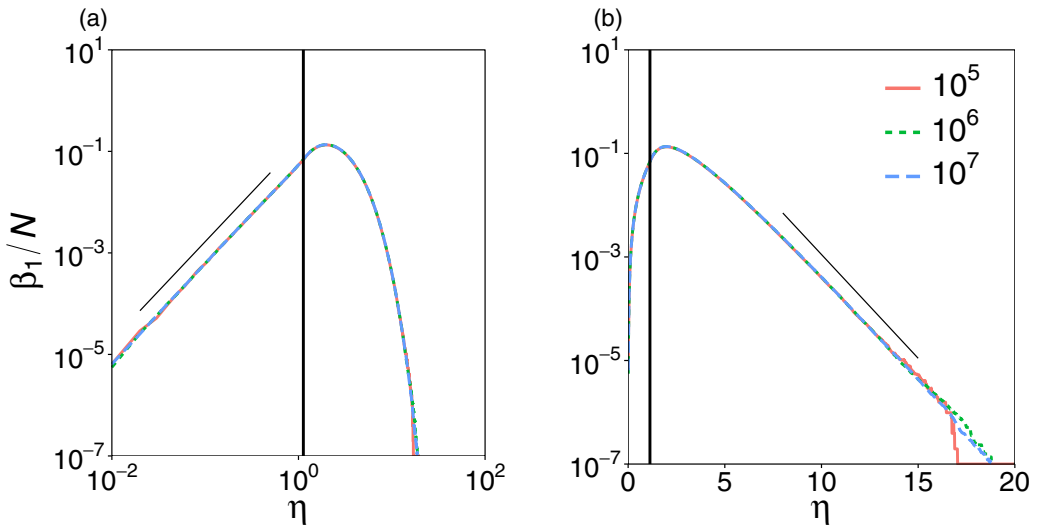

FIG. 4. Mean of β_1/N as a function of η for $N = 10^5$, $N = 10^6$, and $N = 10^7$ disks in continuum percolation with disks with (a) doubly-logarithmic axes and (b) a logarithmic vertical axis. For reference, we show the percolation threshold $\eta_c \approx 1.128$ using a vertical solid line. For visual guidance, we have drawn straight lines in both plots. The slopes of the straight lines are about 1.95 (measured using $\ln(\beta_1/N)/\ln(\eta)$) in panel (a) and about -0.92 (measured using $\ln(\beta_1/N)/\eta$) in panel (b). We calculated these values using a least-squares fit.

suggests the intriguing possibility that, in the limit $N \to \infty$, the longest persisting invariant is born at η_c. It thereby suggests a possible link between PH in continuum percolation with disks and more conventional approaches to studying such percolation.

In Fig. 4, we show how β_1/N changes for $\eta(N,r) \in (0,\infty)$. We observe that the curves collapse onto a single curve for a wide range of $\eta(N,r)$, supporting the linear scaling of β_1 that is predicted by Eq. (4). In Fig. 4(a), we see that β_1/N increases in a manner that seems to resemble a power law until it peaks at a value of η that is larger than the percolation threshold. Recall that in the subcritical regime of the percolation transition, the largest cluster is on the order of $\ln(N)$ (see Sec. III). This suggests that the number of holes per cluster increases rapidly in this regime. From Fig. 4(b), we observe that β_1/N subsequently appears to decay at least exponentially. From this, we deduce that the holes that remain in this regime tend to be small and disappear quickly until eventually the entire unit square $[0,1]^2$ is covered by disks.

VI. CONCLUSIONS AND DISCUSSION

Continuum percolation with disks is a frequently studied variant of continuum percolation, and many of its properties have been uncovered using a combination of theoretical and computational techniques [4–8]. In the present paper, we interpreted the union of potentially overlapping disks generated by continuum percolation with disks as a subspace of $[0,1]^2$ and examined its topological properties near the percolation transition. We computed persistent homology and identified structural changes that cannot be described solely by changes in the sizes of clusters.

We found evidence that the longest persisting invariants are born close to (although seemingly not exactly at) the percolation transition in the limit $N \to \infty$. We also provided numerical confirmation of a theoretical prediction that the first Betti number β_1 scales linearly with respect to the number N of disks, and we characterized β_1 as a function of $\eta(N,r)$.

There are several ways to extend our paper. It will be interesting, for example, to apply PH to higher-dimensional versions of continuum percolation, and one can also ask how the shapes of objects in percolation models affect topological properties. The latter topic is reminiscent of important questions in the study of granular materials [41]. Applying PH to related percolation models, such as random sequential adsorption [19], that incorporate correlations between the placement of disks is also likely to be interesting. More generally, our paper illustrates that it is useful to examine not only the sizes of components in complex systems, but also their shapes, a perspective that we expect to be insightful for many types of phase transitions.

ACKNOWLEDGMENTS

We thank B. J. Stolz and U. Tillmann for helpful comments. L.S. acknowledges support provided by the Engineering and Physical Sciences Research Council (EPSRC) through Grant No. EP/G03706X/1. H.A.H. gratefully acknowledges support through the EPSRC Postdoctoral Fellowship No. EP/KO4196/1 and a Royal Society University Research Fellowship.

[1] A. A. Saberi, Phys. Rep. **578**, 1 (2015).
[2] M. A. Porter and J. P. Gleeson, *Dynamical Systems on Networks: A Tutorial*, Frontiers in Applied Dynamical Systems: Reviews and Tutorials (Springer International Publishing, Cham, Switzerland, 2016), Vol. 4.
[3] H. Kesten, Notices Am. Math. Soc. **53**, 572 (2006).
[4] M. D. Penrose, *Random Geometric Graphs*, Oxford Studies in Probability (Oxford University Press, Oxford, UK, 2003), Vol. 5.
[5] R. Meester and R. Roy, *Continuum Percolation*, Cambridge Tracts in Mathematics (Cambridge University Press, Cambridge, UK, 1996), Vol. 119.
[6] E. N. Gilbert, J. Soc. Ind. Appl. Math. **9**, 533 (1961).
[7] M. Kahle and O. Bobrowski, AMS Contemp. Math. **620**, 201 (2014).
[8] M. Kahle, Discrete Comput. Geom. **45**, 553 (2011).
[9] D. S. Bassett, E. T. Owens, K. E. Daniels, and M. A. Porter, Phys. Rev. E **86**, 041306 (2012).
[10] J. Setford, Models of granular networks in two and three dimensions, Undergraduate Thesis, Department of Physics, University of Oxford (available at http://www.math.ucla.edu/∼mason/research/setford-final.pdf), 2014.
[11] G. Németh and G. Vattay, Phys. Rev. E **67**, 036110 (2003).
[12] C. P. Dettmann and O. Georgiou, Phys. Rev. E **93**, 032313 (2016).
[13] C. Dettmann, O. Georgiou, and P. Pratt, arXiv:1803.04166.
[14] A. R. Kherlopian, T. Song, Q. Duan, M. A. Neimark, M. J. Po, J. K. Gohagan, and A. F. Laine, BMC Syst. Biol. **2**, 74 (2008).
[15] M. Barthélemy, Phys. Rep. **499**, 1 (2011).
[16] M. Barthelemy, *Morphogenesis of Spatial Networks* (Springer International Publishing, Cham, Switzerland, 2018).
[17] E. Katifori, G. J. Szöllősi, and M. O. Magnasco, Phys. Rev. Lett. **104**, 048704 (2010).
[18] A. Pries, T. Secomb, and P. Gaehtgens, Cardiovasc. Res. **32**, 654 (1996).
[19] J. W. Evans, Rev. Mod. Phys. **65**, 1281 (1993).
[20] R. N. Balasubramanian, arXiv:1803.03542.
[21] H. Edelsbrunner and J. L. Harer, *Computational Topology* (AMS, Providence, USA, 2010).
[22] T. Kaczynski, K. Mischaikow, and M. Mrozek, *Computational Homology*, Applied Mathematical Sciences (Springer-Verlag, Berlin, Germany, 2006), Vol. 157.
[23] N. Otter, M. A. Porter, U. Tillmann, P. Grindrod, and H. A. Harrington, EPJ Data Sci. **6**, 17 (2017).
[24] M. Pettini, *Geometry and Topology in Hamiltonian Dynamics and Statistical Mechanics*, Interdisciplinary Applied Mathematics (Springer-Verlag, Berlin, Germany, 2007), Vol. 33.
[25] I. Donato, M. Gori, M. Pettini, G. Petri, S. De Nigris, R. Franzosi, and F. Vaccarino, Phys. Rev. E **93**, 052138 (2016).
[26] F. A. N. Santos, L. C. B. da Silva, and M. D. Coutinho-Filho, J. Stat. Mech. (2017) 013202.
[27] J. Dall and M. Christensen, Phys. Rev. E **66**, 016121 (2002).
[28] S. Mertens and C. Moore, Phys. Rev. E **86**, 061109 (2012).
[29] M. D. Penrose, Ann. Appl. Probab. **26**, 986 (2016).

[30] S. W. Haan and R. Zwanzig, J. Phys. A **10**, 1547 (1977).
[31] J. F. McCarthy, Phys. Rev. Lett. **58**, 2242 (1987).
[32] M. D. Rintoul and S. Torquato, J. Phys. A **30**, L585 (1997).
[33] G. R. Grimmett, *Percolation*, 2nd ed., Grundlehren der mathematischen Wissenschaften (Springer-Verlag, Berlin, Germany, 1999), Vol. 321.
[34] B. Bollobás and O. Riordan, *Percolation* (Cambridge University Press, Cambridge, UK, 2006).
[35] M. E. J. Newman, *Networks*, 2nd ed. (Oxford University Press, Oxford, UK, 2018).
[36] A. Hatcher, *Algebraic Topology* (Cambridge University Press, Cambridge, UK, 2002).
[37] H. Edelsbrunner, D. Kirkpatrick, and R. Seidel, IEEE Trans. Inf. Theory **29**, 551 (1983).
[38] A. Björner, in *Handbook of Combinatorics*, edited by R. L. Graham, M. Grötschel, and L. Lovász (Elsevier Science B.V., Amsterdam, The Netherlands, 1995), Vol. II, pp. 1819–1872.
[39] A. Zomorodian and G. Carlsson, Discrete Comput. Geom. **33**, 249 (2005).
[40] M. Kramár, A. Goullet, L. Kondic, and K. Mischaikow, Phys. Rev. E **90**, 052203 (2014).
[41] L. Papadopoulos, M. A. Porter, K. E. Daniels, and D. S. Bassett, J. Complex Networks (2018); advanced access; available at https://doi.org/10.1093/comnet/cny005.
[42] G. Petri, P. Expert, F. Turkheimer, R. Carhart-Harris, D. Nutt, P. J. Hellyer, and F. Vaccarino, J. R. Soc., Interface **11**, 20140873 (2014).
[43] D. Morozov, DIONYSUS, software available at http://www.mrzv.org/software/dionysus/.
[44] C. Maria, J.-D. Boissonnat, M. Glisse, and M. Yvinec, in *Mathematical Software—ICMS 2014* (Proceedings of the 4th International Congress on Mathematical Software), edited by H. Hong and C. Yap, Lecture Notes in Computer Science (Springer-Verlag, Berlin, Germany, 2014), Vol. 8592, pp. 167–174.